Proceedings of IMECE'03
2003 ASME International Mechanical Engineering Congress
Washington, D.C., November 15–21, 2003

IMECE2003-41481

RADIOFREQUENCY ABLAT ION WITH A GAUSSIAN HEAT SOURCE IN A REALISTIC RECONSTRUCTED HEPATIC GEOMETRY

Ajit K Pandey[1] **Isaac Chang**[2]

Mathew Myers[2] **Rupak K Banerjee**[1,3]

(1) Mechanical Engineering Department
(3) Biomedical Engineering Department
University of Cincinnati,
Cincinnati, OH 45221

(2) Center for Devices and Radiological Health
US Food and Drug Administration,
Rockville, MD 20852

ABSTRACT

This study describes a detailed methodology for modeling a three-dimensional radiofrequency ablation procedure using reconstructed porous tissue geometries. In this study, MRI images of a sectioned liver tissue containing arterial vessels are converted into a finite element mesh. An rf heat source in the form of a spherically symmetric Gaussian distribution, fit from a previously computed profile, is employed. Computations of temperature rise were performed for transient rf procedures in the case where the tumor is located near the bifurcation point of a hepatic artery. Results demonstrate a significant effect due to convective cooling by the large vessels. Substantial asymmetries in the temperature profiles indicate ablation procedures that may achieve adequate tumor destruction in some regions, but that elevate the temperature only minimally in other regions, thereby permitting possible tumor recursion. These critical features of the temperature field are due to the directional nature of the arterial flow and are difficult to capture with models that treat perfusion with a scalar source term in the bioheat equation.

INTRODUCTION

Radio frequency ablation (RFA) is useful for patients with unresectable liver tumors. A treatment session can be of 10-30 minutes duration of active ablation for a 3-5.5 cm spherical zone of necrosis. As tissue temperature rises above 45 C-50 C, proteins get denatured permanently and cell membranes fuse (Chang and Beard, 2002 and Wood *et al.,* 2002). The presence of blood vessels within or near tumors causes the transfer of heat away from the target. The Pennes Bioheat transfer model does not include the presence of large vascular vessels in the tissue domain (Tungjitkusolmun *et al.*, 2002).

Mathematical models are valuable for predicting the temperature rise within the organ during RF ablation, thereby enhancing the likelihood of tumor destruction with minimal damage to surrounding tissue. Models can also be used to predict the optimal setting of operational parameters, such as probe geometry, placement, and power level, for a given tumor location and physiologic geometry.

METHODS

In this study, electric field values are pre-determined for a mplified geometry and are implemented as a Gaussian distributed heat source (Fig. 1A), which remained constant during the ablation.

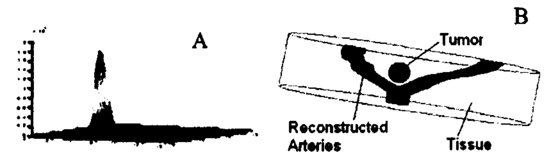

Figure 1: Gaussian Distributed Heat Source depicting the experimental result is shown in Fig. A. Reconstructed bifurcated arteries with surrounding hepatic tissues are shown in Fig. B.

Image Reconstruction and Meshing

A total of 128 images spaced 625 microns apart was obtained from an excised porcine liver segment in a small-bore (45 cm) MRI, controlled by a Tecmag Apollo single channel console running NTNMR software. 3D reconstruction of the geometry is achieved by segmentation, thresholding, and region growing techniques from the segmented MR scans (Mimics, 2003). The excised liver section is of a cylindrical shape (Fig. 1B) with a height of 50 mm and diameter of 170 mm, containing about 600,000 tetrahedral elements (Gambit, 2002). Also shown in Fig. 1B is a hypothetical tumor to be ablated using the rf energy. The tumor is spherical and 1.24 cm in diameter. The bottom of the tumor is located 0.7 cm above the arterial wall at the bifurcation point.

Tissue (Porous Media) Equation

In order to analyze the porous tissue region, the volume elements are considered sufficiently large compared with the length scale of an individual pore. With these assumptions and steady state conditions, the conservation of mass is expressed by the continuity relation,

$$\nabla . \overline{u} = 0 \tag{1}$$

where ∇ is the divergence operator and $\overline{u}$ is the average of the fluid velocity. The momentum equation in tissue domain is expressed by Darcy's law,

$$\overline{u} = -k \nabla p \tag{2}$$

where $\overline{u}$ is the average fluid velocity (m/s), k is the hydraulic conductivity tensor, $k_i = k\mu$ is the permeability (m^2), p is the fluid pore pressure (N/m^2), μ is the fluid viscosity (Ns/m^2).

The following energy equation for porous media is also used for temperature distribution analysis,

$$\left(\rho c_p\right)_e \frac{\partial T}{\partial t} + \left(\rho c_p\right)_e u_j \frac{\partial T}{\partial x_j} = \frac{\partial}{\partial x_j}\left(k_e \frac{\partial T}{\partial x_j}\right) + q_s \tag{3}$$

where T is the temperature (C), ρ is the density (Kg/m^3), c_p is the specific heat (J/kg/K), u is the fluid velocity (m/s), k_e is the thermal conductivity (W/m/K), and q_s is the volumetric Gaussian heat source (W/m^3). The effective properties are related to fluid and solid matrix properties by the relations,

$$\left(\rho c_p\right)_e = \phi \rho c_p + (1-\phi)\left(\rho c_p\right)_s \tag{4}$$

$$(k)_e = \phi k + (1-\phi)(k)_s \tag{5}$$

where ϕ is the porosity, properties without subscripts are those of the blood and properties with the subscript '*s*' are those of the tissue solid.

For the arterial (continuum blood flow) region, the standard mass, momentum, and energy equation are used.

Heat Source and Boundary conditions

In the present study, the RF probe is modeled as a Gaussian distributed spherical heat source for a tissue volume of 0.52×10^{-6} m^3. The three dimensional heat source has spherical symmetry and is a function of radius only. The average integrated value of the Gaussian heat source is 14.1×10^5 W/m^3. The Gaussian heat source equation in Cartesian coordinate system is,

$$Q(x, y) = A\left(e^{-\left(a(x-x_m)^2 + b(x-x_m)(y-y_m) + c(y-y_m)^2\right)}\right) \qquad (6)$$

where x, y, and z are the nodal coordinate values (cm), A is the peak value of Gaussian; a, b, and c decide the shape of the Gaussian, x_m and y_m are the mean value of the x and y coordinates (cm) respectively. A, a, b, c, x_m, y_m are evaluated by the Nelder-Mead scheme (Matlab, 2002).

The boundary conditions imposed on all external surfaces is zero heat flux except at the inlet of the artery and the tissue near it, where a constant temperature of 37 C is used. For flow, a stress free boundary condition is used at all boundaries except at the arterial inlet. Since 25% of the total blood volume passes through liver body, basal inlet velocity of 13.8 cm/s (an equivalent perfusion of 0.3 ml/min/(ml of tissue)) is calculated and imposed at the artery inlet. Also hyperemic inlet velocities of 27.8 and 41.4 cm/s are imposed to obtain different values of perfusion (0.65 and 1.01 ml/min/(ml of tissue), respectively) and convection. A permeability of 10^{-10} m^2 was required to achieve the defined level of perfusion. The tissue and blood properties are taken from Duck, 1990.

RESULTS AND DISCUSSION

The axial temperature profile is displayed in Figs. 2 A-D. Here the temperature rise is plotted for the case of no blood flow (Fig. 2A) and arterial inlet velocities of 13.8 cm/s (Fig. 2B), 27.6 cm/s (Fig. 2C), and 41.4 cm/s (Fig. 2D). Ablation times of 1, 4, 8, and 32 minutes are considered. In the case of no blood flow, the maximum temperature rise (as a function of axial position) for a 32-minute ablation time is 52 C (Fig. 2A). The profile width, defined as the distance over which the temperature rise drops to half the peak value, is approximately 5.5 mm. In the presence of blood flow, the maximum temperature rise for a 32-minute ablation is 47 C for lowest arterial velocity (Fig. 2B) and 38 C for the highest (Fig. 2D). The corresponding profile widths, measured on the bottom side of the tumor, vary from approximately 5 mm for the lowest arterial velocity to 3 mm for the highest.

For nonzero arterial flow (Figs. 2B, 2C, 2D), the location of maximum tumor temperature shifts upward relative to the no-flow case. For the 32-minute heating duration, the shift increases with arterial flow rate, from approximately 0.5 mm at the lowest velocity to 1.2 mm for the highest arterial flow. The location of the maximum temperature also shifts upward with time; this trend is most evident at high flow rates (Figs. 2C, 2D). The important asymmetry exhibited in Fig. 2 is a natural product of direct physical modeling and difficult to capture using scalar perfusion models. In contrast with the axial dependence of the temperature field, the temperature profile is symmetric in the x- and y-directions.

The temperature plots of Fig. 2 demonstrate the importance of accurately modeling the effects of convection when the rf heat source is concentrated near a large vessel. While the temperature rise at the center of the tumor may be high enough to achieve destruction, tumor regions located nearest the vessel boundary experience minimal temperature elevation. Thus model predictions can identify locations where tumor recursion is likely without further intervention.

The present model does not account for thermally significant vessels other than the bifurcating artery. Hence, the model is most useful for providing insight into rf ablation when convective heat transfer is dominated by the effects due to a single vessel. The present model also employs a highly simplified, spherically symmetric heat source. Future generations of the model will include a more realistic electrical-field configuration, such as that due to a 4tine probe considered by Tungjitkusolmun et al. (2002).

REFERENCES

Chang I. and Beard B., 2002, *Medical Engrng & Physics*, 24, pp. 633-640.

Duck F., 1990, "*Physical properties of tissue*," Academic Press, NewYork, pp. 167-223.

Fidap/Gambit Manual, 2002, Fluent Inc., Lebanon, NH.

Matlab Manual, ver. 6.5, 2002, Mathworks Inc., Natick, MA.

Mimics Manual, ver. 7.1, 2003, Materialise Inc., Ann Arbor, MI.

Arkin H *et al*, 1994, *IEEE Trans Biomed Eng.*, Feb; 41(2), pp. 97-107. Review.

Tungjitkusolmun S. *et al.*, 2002, *IEEE Trans Biomed Eng.*, Vol. 49, pp. 3-9.

Wood, Bradford J. *et al.*, Jan 15, 2002, *Cancer*, pp. 443-451.

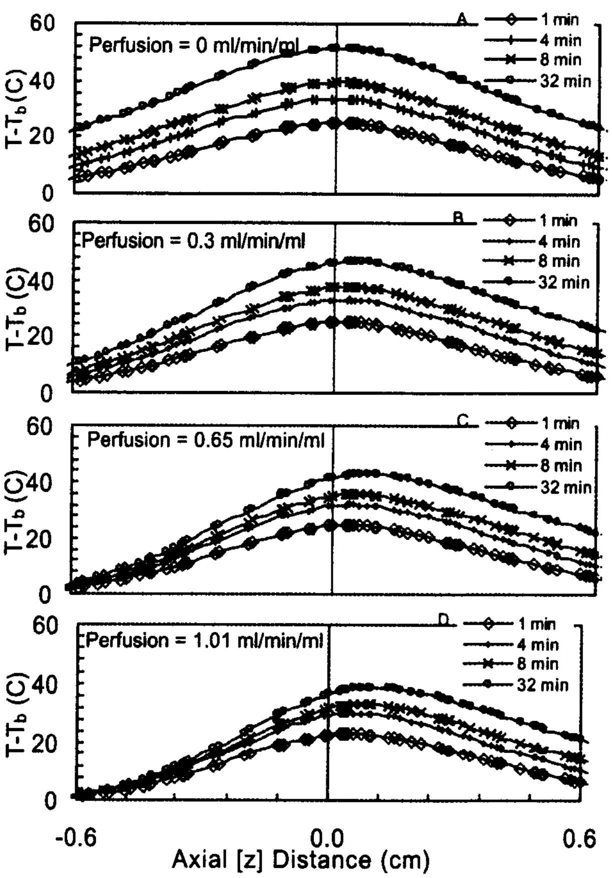

Figure 2: Temporal and spatial distribution of the temperature for probe located at r = 0 cm and the effect of blood perfusion of 0, 0.3, 0.65 and 1.01 ml/min/(ml of tissue) on temperature is shown in Figs. A through D respectively.